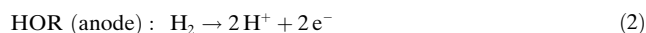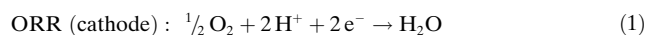**Oxygen Reduction**

Dramatic Increase in the Oxygen Reduction Reaction for Platinum Cathodes from Tuning the Solvent Dielectric Constant**

Alessandro Fortunelli,* William A. Goddard,* Yao Sha, Ted H. Yu, Luca Sementa, Giovanni Barcaro, and Oliviero Andreussi

Abstract: *Hydrogen fuel cells (FC) are considered essential for a sustainable economy based on carbon-free energy sources, but a major impediment are the costs. First-principles quantum mechanics (density functional theory including solvation) is used to predict how the energies and barriers for the mechanistic steps of the oxygen reduction reaction (ORR) over the fcc(111) platinum surface depend on the dielectric constant of the solvent. The ORR kinetics can be strongly accelerated by decreasing the effective medium polarizability from the high value it has in water. Possible ways to realize this experimentally are suggested. The calculated volcano structure for the dependence of rate on solvent polarization is considered to be general, and should be observed in other electrochemical systems.*

Hydrogen fuel cells (FC) are considered as essential for a sustainable economy based on carbon-free energy sources,[1] but a major impediment are the costs. In these electrochemical devices, H_2 (generated e.g. from solar energy conversion) reacts with O_2 to produce electricity via the cathode oxygen reduction reaction (ORR)[2–5] and the anode hydrogen oxidation reaction (HOR):

$$\text{ORR (cathode)}: \; \tfrac{1}{2}\,O_2 + 2\,H^+ + 2\,e^- \rightarrow H_2O \tag{1}$$

$$\text{HOR (anode)}: \; H_2 \rightarrow 2\,H^+ + 2\,e^- \tag{2}$$

[*] A. Fortunelli, L. Sementa, G. Barcaro
CNR-ICCOM and IPCF, Consiglio Nazionale delle Ricerche
via Giuseppe Moruzzi 1, 56124 Pisa (Italy)
E-mail: alessandro.fortunelli@cnr.it

A. Fortunelli, W. A. Goddard, Y. Sha, T. H. Yu
Materials and Process Simulation Center
California Institute of Technology
MC 139-74, Pasadena, CA 91125 (USA)
E-mail: afloer@caltech.edu
       wag@wag.caltech.edu

O. Andreussi
University of Pisa, Dipartimento Chimica & Chimica Industriale
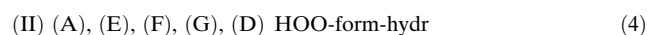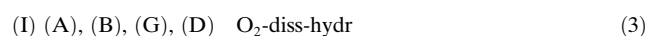Via Risorgimento 35, 56126 Pisa (Italy)

Despite the large thermodynamic driving force (68.36 kcal mol^{-1}) associated with H_2 combustion, hydrogen fuel cells exhibit very slow kinetics, even on the best (platinum-based) catalyst electrodes. Indeed the ORR rate, which is ≈ 400 times slower than the anode HOR,[1–5] is the critical bottleneck in making Hydrogen FCs economic. On platinum-based cathodes, this is not due to paucity of catalytic sites, since the catalytically active area for Pt and Pt-alloy nanoparticles dispersed, say, onto high-surface-area carbon black support is at least 20-30 $m^2 g_{Pt}^{-1}$, reaching 100 $m^2 g_{Pt}^{-1}$ on optimized cells.[1] Rather, the abominably slow kinetics must be due to a significant reaction energy barrier in the overall ORR process.

Here we use first-principles quantum mechanics (density functional theory including solvation) for the fcc Pt(111) surface, a model of Pt-based catalysis. Building on the results of several recent studies,[5–9] we investigate the effect of the solvent environment on the ORR mechanism and energetics. We show that the reaction energy barriers of the various reaction steps involved in the ORR on Pt(111) depend strongly on the solvent dielectric constant. This suggests that properly tuning the solvent dielectric constant can lead to a significant acceleration of the ORR kinetics. Indeed the calculations suggest that achieving this optimum dielectric constant could increase the ORR by a factor of ≈ 600. Such a dramatic increase in the rate for ORR could reduce the cost of the current generation Hydrogen FC by a factor of 2, since half the cost is due to the Pt used in the catalyst. We also make some suggestions on how this might be realized in practice. Our analysis shows that one can generally expect a volcano curve[10] for the overall reaction rate as a function of the solvent dielectric constant, suggesting that examining the experimental kinetics as a function of the effective dielectric constant provides an effective tool to optimize the kinetics for such catalytic processes.

Our calculations are based on density functional theory (DFT), employing the exchange-correlation functional proposed by Perdew, Burke and Ernzerhof (PBE)[11] and the solvation approach for periodic slabs developed recently.[9] We use the SeqQuest[12] implementation with an optimized double-ζ plus polarization Gaussian type basis set contracted from calculations on the most stable unit cell of the pure elements. Angular-momentum-projected norm-conserving nonlocal effective core potentials[13–16] are used to replace the core electrons. Thus, the Pt atom is described with 16 explicit electrons (six 5p, one 6s, and nine 5d in the ground state). The real space grid density is 5 points/Å, while the reciprocal space grid is $(5 \times 5 \times 0)$ for slab calculations. All calculations allowed the up-spin orbitals to be optimized

independently of the down spin orbitals (spin-unrestricted DFT). The Pt(111) surface is modelled within a periodic model using a slab made of four Pt layers, each containing 9 metal atoms in the unit cell (3×3 cells): the bottom two Pt layers are frozen in the crystal positions using the experimental equilibrium value of the bulk Pt lattice constant (2.775 Å), whereas the top two layers are free to relax together with the adsorbed species. The calculation of solvation effects employs a continuum model[17,18] based on the Poisson–Boltzmann approximation (APBS).[19,20] Reaction pathways are determined using the Nudged Elastic Band (NEB)[21-23] method, and solvent effects are included a posteriori for each point along the path by using the continuum model. When changing the dielectric constant of the medium (ε), we assume that cavitation and dispersion/repulsion contributions to the solvation energy do not change,[17,18] and focus on the electrostatic polarization term only. Here variations of ε from 78 (appropriate for water in standard conditions) to 1 (vacuum) are considered. In the Supporting Information (SI) we validate the computational approach by comparison against a completely different code[24] and solvation model.[25-27] It should be noted that the solvent dielectric constant at the interface may be different from its bulk value.[28] However for the water/Pt(111) case we found that the resulting effective dielectric constant is still sizable: around 28 (unpublished work by T. Pascal and W. A. Goddard III). Moreover, in realistic ORR conditions the massive presence of diverse adsorbates on Pt(111) is expected to disrupt self-organization of water at the interface with the metal as predicted in idealized conditions, so that a bulk water dielectric constant can be reasonably assumed. The Continuum models used here provide an effective description of solvation energetics that allow us to examine quickly the overall effects. Having established that it is important to have a low dielectric constant for the rate determining step, we set the stage for carrying out more detailed atomistic studies including explicit description of hydrogen bonding.

The basic reaction steps (A–G) by which the ORR is realized on Pt(111) are shown in Figure 1, with each step named by a self-explanatory label. As discussed in Ref. [9], two mechanisms (as sequences of individual reaction steps) are available to realize the ORR on Pt(111) (the nomenclature of reaction steps is as in Figure 1):

$$(I) \quad (A), (B), (G), (D) \quad O_2\text{-diss-hydr} \qquad (3)$$

$$(II) \quad (A), (E), (F), (G), (D) \quad HOO\text{-form-hydr} \qquad (4)$$

These two mechanisms differ only in that the O_2 activation step (B) of (I) is replaced by the (E) + (F) steps of (II). Other possible mechanisms such as H_2O_2 formation are not favourable on Pt(111), being at high energy, see for example, Figure 3 in Ref. [29] and experimentally accounting for at most 5% of the total process even at high potential, see Figure 6 in Ref. [30]. We also assume that the hydronium ion H^+ takes part to the reaction as an adsorbed H-adatom (coloured white in Figure 1) in a Langmuir-Hinshelwood mechanism rather than directly as a solvated species in a Eley-Rideal mechanism.[5] This is computationally convenient,
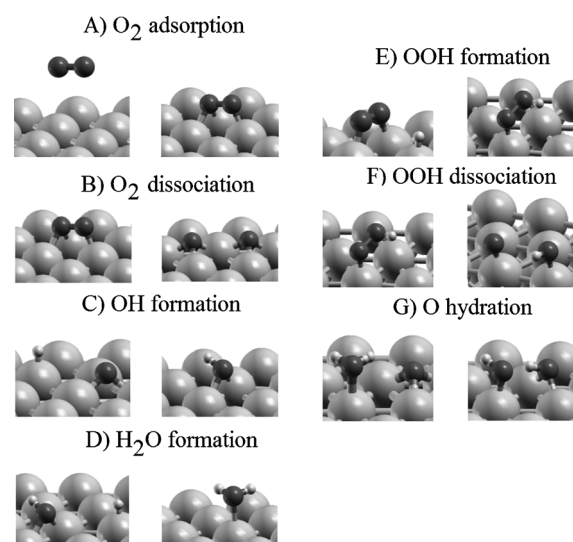

Figure 1. Basic reaction steps of the ORR on Pt(111), see Ref. [9] H, O, and Pt atoms in white, dark gray, and light gray, respectively.

A) O_2 adsorption
B) O_2 dissociation
C) OH formation
D) H_2O formation
E) OOH formation
F) OOH dissociation
G) O hydration

simplifies our simulations by avoiding issues connected with the description of charged species in periodic systems, and is justified by the detailed analysis of Ref. [5] in which a Eley-Rideal path is shown to be replaced by a Langmuir-Hinshelwood one at realistic values of the electrode potential. Moreover, the energy difference between H-adsorbed and the proton in solution (which is 0.40 eV experimentally and −0.44 eV from our approach[31]) becomes more negative as the polarizability of the medium is decreased, thus further favouring a Langmuir-Hinshelwood mechanism. The crucial point derived from the analysis in Ref. [9] is that in strongly polarizable and high dielectric constant solvents (such as water) the O_2 dissociation step, Figure 1 B, which is usually assumed to be the rate-determining-step (rds), is instead essentially barrier-less, due to the large energy gained by hydrating the resulting oxygen adatoms. This annihilates the barrier to break the strong oxygen-oxygen bond. In such conditions the rds becomes the oxygen hydration step, Figure 1 G, which is the reverse of hydroxyl disproportionation. Thus the actual ORR mechanism switches from the HOO-form-hydr mechanism (II) favored in the gas phase to the O_2-diss-hydr mechanism (I) favored in water. The resulting energy barrier for the rds of ORR in water ($\varepsilon = 78$) is ≈ 0.5 eV, compared to ≈ 0.3 eV for gas phase ($\varepsilon = 1$).[9] Here the gas phase is taken to represent the Teflon-Pt interface for Nafion electrolyte or a three-phase surface. Of course, this analysis for the gas phase neglects the necessity of a diffusion medium to provide for H^+ mobility while closing the electrochemical cycle. It should be noted that the O_2-diss-hydr mechanism only depends on the electrode potential in the H_2O formation step (D). If—as usually assumed[3,5]—we include the effect of the electrode potential by shifting by the term $+eV$ (with e the unit charge and V the potential) the energy of intermediates following a one-electron reduction, the fact that step (D) is thermodynamically favored by 0.8 eV in our approach implies that it cannot be rate-determining up to realistic values of the electrode potential (up to 1.1 V).

In Figure 2a we report the behaviour of the energy barriers for the rate-determining steps of the ORR as a function of the logarithm of the dielectric constant of the environment (ε) for both mechanisms (I) and (II) as obtained through our approach (more details can be found in the Supplementary Information). This plot suggests that by appropriate modifications in the solvent polarity one could decrease the energy barrier of the ORR rds significantly from the value in water ($\approx 0.5\,\mathrm{eV}$) to $\approx 0.30\,\mathrm{eV}$, which at the current operating temperature of $85\,°\mathrm{C}$ would correspond to a rate acceleration by a factor of ≈ 650 as the solvent dielectric constant is reduced from the high value it has in water. At $27\,°\mathrm{C}$ (room temperature) the rate enhancement would be ≈ 2300 (see Figure 2b for a plot of the relative rates for the two processes as a function of the logarithm of ε). Thus by changing the effective solvent dielectric constant, we should be able to increase the ORR rate while reducing the reaction temperature. This behaviour is consistent in general terms with the Sabatier principle of catalysis,[32] which states that optimizing the performance of any given catalytic system

requires a balance between conflicting requirements, so that the optimal catalyst is a compromise between strong and weak energetics, in our case achieved by adjusting the dielectric properties of the environment (H^+ formation at the anode needs to be considered for obtaining the complete volcano plot).

To translate these predictions into specific suggestions for experimental testing we need to answer the question of how to achieve a reduction in ε without degrading other solvent characteristics necessary for the electrochemical process to occur efficiently such as ion and mass transport. It might seem that an optimum dielectric constant of 2 or 3 is too low for a practical system, but as suggested in Ref. [9], this might be achievable for the case of Nafion by a precise engineering of the Teflon-Pt interface distance at the nanoscale as to reduce the H_2O concentration to about 1/2 monolayer, which still allows the proton migration to the Pt surface through the hydrophilic channels of Nafion while allowing enough H_2O in the hydrophobic region to promote reaction G (hydration of surface O). Alternatively we could mix water with other, less polarizable solvents using empirical mixing rules for predicting the resulting ε[33,34] so as to orient the choice of co-solvents that would lead to the optimum dielectric constant. Indeed, by modifying such co-solvent properties as molecular size, polarizability and ability of creating H-bonds, we expect to be able to choose the optimum co-solvent features to perturb the network of H-bonds next to the metallic surface[35,36] without destroying it. Thus we might simultaneously achieve: 1) a sizable H^+ mobility and O_2 diffusivity, and 2) beneficial solvation/desolvation fluctuations in the electronic and librational polarization fields around the reactants to realize the optimal compromise between the opposite behavior with ε of the energy barriers of the O_2-dissociation (B or EF) and O-hydration (G) steps. This subtle interplay of various factors and phenomena makes the situation complex and sensitive to the atomistic details of the solvent medium, so that mapping of the experiments onto our volcano plot may provide the guide sought for the ORR, opening pathways way for novel combinations of materials.

A comparison of the energetics of the ORR using a different code[24] and solvation model[25], and the energy barriers of the ORR reaction steps as a function of the solvent dielectric constant can be found in the Supporting Information.
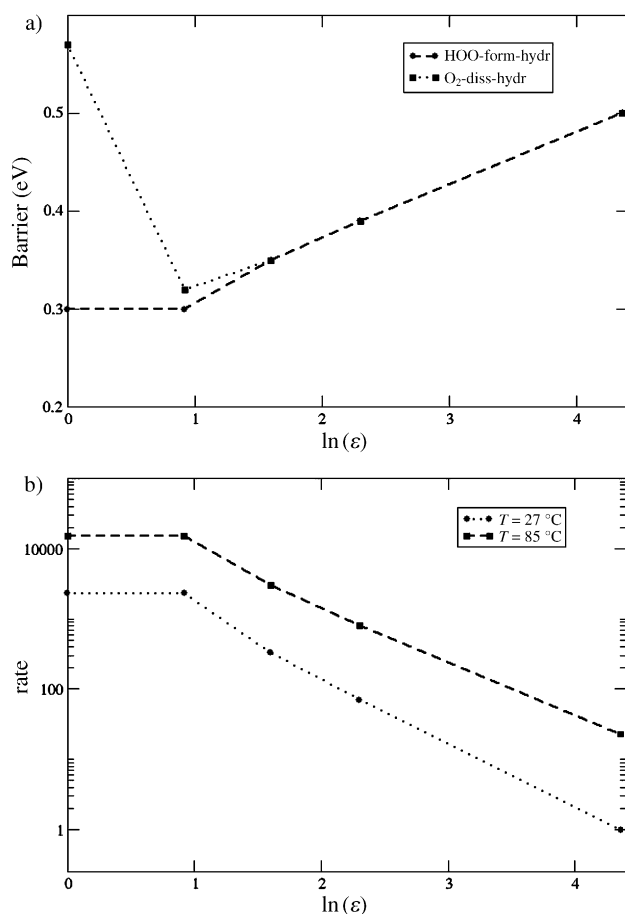
Figure 2. a) Energy barriers of the rate-determining steps of the ORR on Pt(111) for the O_2-diss-hydr mechanism (dotted line), and the HOO-form-hydr mechanism (dashed line), as a function of the logarithm of the dielectric constant of the solvent (ε); b) rate enhancement in logarithmic scale with respect to the rate in water at $27\,°\mathrm{C}$ as obtained at temperature of $27\,°\mathrm{C}$ (dotted curve) and $85\,°\mathrm{C}$ (dashed curve)—Arrhenius prefactors are assumed to be the same for the two mechanisms.

[1] M. K. Debe, *Nature* **2012**, *486*, 43–51.
[2] N. M. Marković, T. J. Schmidt, V. Stamenković, P. N. Ross, *Fuel Cells* **2001**, *1*, 105–116.
[3] J. K. Nørskov, J. Rossmeisl, A. Logadottir, L. Lindqvist, J. R. Kitchin, T. Bligaard, H. Jonsson, *J. Phys. Chem. B* **2004**, *108*, 17886–17892.
[4] M. J. Janik, C. D. Taylor, M. Neurock, *J. Electrochem. Soc. B* **2009**, *156*, B126–135.

[5] J. A. Keith, T. Jacob, *Angew. Chem.* **2010**, *122*, 9711–9716; *Angew. Chem. Int. Ed.* **2010**, *49*, 9521–9525, and references therein.

[6] T. Zhang, A. B. Anderson, *Electrochim. Acta* **2007**, *53*, 982–989.

[7] V. Rai, M. Aryanpour, H. Pitsch, *J. Phys. Chem. C* **2008**, *112*, 9760–9768.

[8] J. Greeley, J. K. Nørskov, *J. Phys. Chem. C* **2009**, *113*, 4932–4939.

[9] Y. Sha, T. H. Yu, B. V. Merinov, P. Shirvanian, W. A. Goddard, *J. Phys. Chem. Lett.* **2011**, *2*, 572–576.

[10] J. K. Nørskov, T. Bligaard, J. Rossmeisl, C. H. Christensen, *Nat. Chem.* **2009**, *1*, 37–46.

[11] J. Perdew, K. Burke, M. Ernzerhof, *Phys. Rev. Lett.* **1996**, *77*, 3865–3868.

[12] P. Schultz, SeqQuest code project; Sandia National Laboratories: Albuquerque, NM (http://www.cs.sandia.gov/~paschul/Quest/).

[13] C. F. Melius, W. A. Goddard, *Phys. Rev. A* **1974**, *10*, 1528–1540.

[14] C. F. Melius, B. D. Olafson, W. A. Goddard, *Chem. Phys. Lett.* **1974**, *28*, 457–462.

[15] A. Redondo, W. A. Goddard, T. C. Mcgill, *Phys. Rev. B* **1977**, *15*, 5038–5048.

[16] D. R. Hamann, *Phys. Rev. B* **1989**, *40*, 2980–2987.

[17] J. Tomasi, M. Persico, *Chem. Rev.* **1994**, *94*, 2027–2094.

[18] C. Cramer, D. Truhlar, *Chem. Rev.* **1999**, *99*, 2161–2200.

[19] D. J. Tannor, B. Marten, R. Murphy, R. A. Friesner, D. Sitkoff, A. Nicholls, M. Ringnalda, W. A. Goddard, B. Honig, *J. Am. Chem. Soc.* **1994**, *116*, 11875–11882.

[20] N. Baker, D. Sept, S. Joseph, M. Holst, J. McCammon, *Proc. Natl. Acad. Sci. USA* **2001**, *98*, 10037–10041.

[21] G. Mills, H. Jonsson, *Phys. Rev. Lett.* **1994**, *72*, 1124–1127.

[22] G. Mills, H. Jonsson, G. K. Schenter, *Surf. Sci.* **1995**, *324*, 305–337.

[23] G. Henkelman, B. P. Uberuaga, H. Jonsson, *J. Chem. Phys.* **2000**, *113*, 9901–9904.

[24] P. Giannozzi et al., *J. Phys.: Condens. Matter.* **2009**, *21*, 395502.

[25] O. Andreussi, I. Dabo, N. Marzari, *J. Chem. Phys.* **2012**, *136*, 064102.

[26] D. A. Scherlis, J. L. Fattebert, F. Gygi, M. Cococcioni, N. Marzari, *J. Chem. Phys.* **2006**, *124*, 074103.

[27] J. L. Fattebert, F. Gygi, *J. Comput. Chem.* **2002**, *23*, 662–666.

[28] "A Phase Transition Induced by Water Reorientation at Electrode Interfaces": L. Blum, D. A. Huckaby in *New Kinds of Phase Transitions: Transformations in Disordered Substances* (Eds.: V. V. Brazhkin, S. V. Buldyrev, V. N. Ryzhov, H. E. Stanley), Proc. NATO Advanced Research Workshop, Volga River, May 2001, Kluwer, Dordrecht, **2002**, p. 131.

[29] T. H. Yu, Y. Sha, W.-G. Liu, B. V. Merinov, P. Shirvanian, W. A. Goddard III, *J. Am. Chem. Soc.* **2011**, *133*, 19857–19863.

[30] C. M. Sánchez-Sánchez, A. J. Bard, *Anal. Chem.* **2009**, *81*, 8094–8100.

[31] Y. Sha, T. H. Yu, B. V. Merinov, W. A. Goddard, *J. Phys. Chem. C* **2012**, *116*, 6166–6173.

[32] P. Sabatier, *Ber. Dtsch. Chem. Ges.* **1911**, *44*, 1984–2001.

[33] G. Oster, *J. Am. Chem. Soc.* **1946**, *68*, 2036.

[34] P. Wang, A. Anderko, *Fluid Phase Equilib.* **2001**, *186*, 103–122.

[35] A. Poissier, S. Ganeshan, M. V. Fernandez-Serra, *Phys. Chem. Chem. Phys.* **2011**, *13*, 3375–3384.

[36] T. A. Pascal, W. A. Goddard, *J. Phys. Chem. B* **2012**, *116*, 13905–13912.